ICAS 2021 SHANGHAI
International Council of the Aeronautical Sciences
32nd Congress of the International Council of the Aeronautical Sciences
September 6-10, 2021
Pudong Shangri-La, Shanghai, China

AIRCRAFT AUTOPILOT DESIGN USING ASYMMETRIC VARIABLE-SPAN WING MORPHING

Jihoon Lee[1], Seong-hun Kim[1], Seungyun Jung[1], Hanna Lee[1] & Youdan Kim[1,2]

[1]Department of Aerospace Engineering, Seoul National University, Seoul 08826, Republic of Korea
[2]Institute of Advanced Aerospace Technology, Seoul National University, Seoul 08826, Republic of Korea

Abstract

In this study, a flight control system is designed for an asymmetric variable-span morphing aircraft. The generic transport model is used to obtain a morphing aircraft model by incorporating the damage information. The integrated flight control system is designed based on nonlinear dynamic inversion and time-scale separation. It is shown that asymmetric span morphing can be used for roll control, while symmetric morphing can be used to either optimize flight performance or directly control aerodynamic forces. Numerical simulation results demonstrate the effectiveness of the proposed scheme.

Keywords: Morphing aircraft, nonlinear dynamic inversion, flight control, autopilot, variable-span wing

Nomenclature

η_L, η_R	=	left and right morphing variables
η_s, η_a	=	symmetric and asymmetric morphing variables
x, y, z	=	north, east, and down positions
V	=	true airspeed
χ, γ	=	horizontal and vertical flight path angles
μ, α, β	=	bank angle, angle of attack, and sideslip angle
p, q, r	=	roll, pitch, and yaw rates
X_A, Y_A, Z_A	=	body-axis aerodynamic forces
X_T, Y_T, Z_T	=	body-axis thrust forces
l_A, l_A, l_A	=	body-axis aerodynamic moments
l_T, l_T, l_T	=	body-axis thrust moments
g	=	gravitational acceleration
m, J	=	mass and moment of inertia
ρ, S	=	atmospheric density and planform area
$\bar{c}, b$	=	mean aerodynamic chord and wing span
C_X, C_Y, C_Z	=	aerodynamic force coefficients
C_l, C_m, C_n	=	aerodynamic moment coefficients
x_{cp}, y_{cp}, z_{cp}	=	center of pressure location
x_{cg}, y_{cg}, z_{cg}	=	center of gravity location
T_L, T_R	=	left and right thrust
T	=	total thrust
θ_L, θ_R	=	engine pitch angles
ψ_L, ψ_R	=	engine yaw angles
$\delta_t, \delta_e, \delta_r$	=	engine throttle and elevator and rudder deflections
$K_{P_1}, K_{I_1}, K_{D_1}$	=	velocity loop gains
$K_{P_2}, K_{I_2}, K_{D_2}$	=	attitude loop gains
$K_{P_3}, K_{I_3}, K_{D_3}$	=	angular velocity loop gains

Figure 1 – Generic transport model tail number T2 [8].

1. Introduction

Morphing aircraft are advanced aerial platforms that are capable of in-flight large-scale shape changes, which enable them to adapt to mission environment change. Also, morphing can be utilized as an effective way to control the airframe in addition to the conventional flap-type control surfaces. However, existing studies on the morphing aircraft have been focused mainly on realizing various morphing mechanisms and demonstrating the effectiveness of the design. Many practical and theoretical issues have to be addressed for morphing technologies to be incorporated with integrated flight control systems.

Various morphing strategies and their aerodynamic effects have been investigated in many studies including span, sweep, camber, pitch, twist, gull, and folding morphing [1]. Telescoping, chord extension, variable-sweep, and airfoil morphing strategies were compared in [2]. It was demonstrated that morphing can be used for roll control [3, 4, 5, 6, 7]. Now, variable-span morphing is known as one of the most cost-effective morphing strategies.

In this study, a flight control system is designed for asymmetric variable-span morphing aircraft. The damage effects of the NASA generic transport model tail number T2 (GTM-T2), shown in Fig. 1. are adapted to construct a morphing aircraft model. The integrated flight control system is designed based on nonlinear dynamic inversion (NDI) and time-scale separation. It is shown that asymmetric span morphing can be used for roll control, while symmetric morphing can be used to either optimize flight performance or directly control aerodynamic forces. Numerical simulation results demonstrate the effectiveness of the proposed scheme.

2. Aircraft Model

Based on the GTM-T2 [8], an asymmetric variable-span morphing aircraft model is constructed. The GTM-T2 contains the damage model for the case when the left wingtip is removed. The increments to the centers of gravity, moments of inertia, and aerodynamic coefficients are given. In this study, a variable-span model is obtained using the increments and the symmetry of the airframe, where it is assumed that the left and right wingtips can be telescoped. The morphing variables η_L and η_R are introduced, which represent each wing's telescoping ratio ranging from 0 (0%) to 1 (25%). Then, symmetric and asymmetric morphing variables are defined for control design as

$$\eta_s = \frac{\eta_L + \eta_R}{2} \tag{1}$$

$$\eta_a = \frac{\eta_L - \eta_R}{2} \tag{2}$$

It is also assumed that the variations in the aerodynamic coefficients between both ends, shortest and longest version of the variable-span, can be approximated through linear interpolation with acceptable errors. Note that the center of gravity and the moment of inertia can be exactly obtained using the model information. It can be shown that the center of gravity is obtained as a linear function of the morphing variables and the moment of inertia is obtained as a quadratic function of the morphing variables.

2.1 Equations of Motion

In this study, it is assumed that the variable-span morphing process is slow enough so that the airframe can be treated as a rigid body. The flight dynamics of a morphing aircraft can be described as follows [9],

$$\begin{bmatrix}\dot{x}\\ \dot{y}\\ \dot{z}\end{bmatrix} = \begin{bmatrix}V\cos\chi\cos\gamma\\ V\cos\chi\sin\gamma\\ -V\sin\gamma\end{bmatrix} \tag{3}$$

$$\begin{bmatrix}\dot{V}\\ \dot{\chi}\\ \dot{\gamma}\end{bmatrix} = \begin{bmatrix}\frac{1}{\mathrm{m}} & 0 & 0\\ 0 & \frac{1}{\mathrm{m}V\cos\gamma} & 0\\ 0 & 0 & -\frac{1}{\mathrm{m}V}\end{bmatrix}\left(T_{VB}\begin{bmatrix}X_A+X_T\\ Y_A+Y_T\\ Z_A+Z_T\end{bmatrix} + T_{VN}\begin{bmatrix}0\\ 0\\ \mathrm{m}g\end{bmatrix}\right) \tag{4}$$

$$\begin{bmatrix}\dot{\mu}\\ \dot{\alpha}\\ \dot{\beta}\end{bmatrix} = \begin{bmatrix}\cos\alpha\cos\beta & 0 & \sin\alpha\\ \sin\beta & 0 & 0\\ \sin\alpha\cos\beta & 0 & -\cos\alpha\end{bmatrix}^{-1}\left(-T_{BV}\begin{bmatrix}-\dot{\chi}\sin\gamma\\ \dot{\gamma}\\ \dot{\chi}\cos\gamma\end{bmatrix} + \begin{bmatrix}p\\ q\\ r\end{bmatrix}\right) \tag{5}$$

$$\begin{bmatrix}\dot{p}\\ \dot{q}\\ \dot{r}\end{bmatrix} = J^{-1}\left(\begin{bmatrix}l_A+l_T\\ m_A+m_T\\ n_A+n_T\end{bmatrix} - \begin{bmatrix}p\\ q\\ r\end{bmatrix}\times J\begin{bmatrix}p\\ q\\ r\end{bmatrix}\right) \tag{6}$$

where

$$T_{VB} = T_{BV}^T = \begin{bmatrix}\cos\alpha\cos\beta & \sin\beta & \sin\alpha\cos\beta\\ -\cos\alpha\sin\beta\cos\mu+\sin\alpha\sin\mu & \cos\beta\cos\mu & -\sin\alpha\sin\beta\cos\mu-\cos\alpha\sin\mu\\ -\cos\alpha\sin\beta\sin\mu-\sin\alpha\cos\mu & \cos\beta\sin\mu & -\sin\alpha\sin\beta\sin\mu+\cos\alpha\cos\mu\end{bmatrix} \tag{7}$$

$$T_{VN} = \begin{bmatrix}\cos\chi\cos\gamma & \sin\chi\cos\gamma & -\sin\gamma\\ -\sin\gamma & \cos\gamma & 0\\ \cos\chi\sin\gamma & \sin\chi\sin\gamma & \cos\gamma\end{bmatrix} \tag{8}$$

In the above equations, flat-Earth and no-wind conditions are assumed. The equations of motion are represented in the velocity coordinate, it is focused on the spatial motion of the morphing aircraft when using morphing. In addition, symmetric morphing can be used for direct force control together with thrust, which can enable partial position-attitude separation control.

2.2 Aerodynamic Model

The aerodynamic forces and moments are obtained as follows,

$$\begin{bmatrix}X_A\\ Y_A\\ Z_A\end{bmatrix} = \frac{1}{2}\rho V_T^2 S\begin{bmatrix}C_X\\ C_Y\\ C_Z\end{bmatrix} \tag{9}$$

$$\begin{bmatrix}l_A\\ m_A\\ n_A\end{bmatrix} = \begin{bmatrix}0 & -(z_{cp}-z_{cg}) & y_{cp}-y_{cg}\\ z_{cp}-z_{cg} & 0 & -(x_{cp}-x_{cg})\\ -(y_{cp}-y_{cg}) & x_{cp}-x_{cg} & 0\end{bmatrix}\begin{bmatrix}X_A\\ Y_A\\ Z_A\end{bmatrix} + \frac{1}{2}\rho V^2 S\begin{bmatrix}b & 0 & 0\\ 0 & \bar{c} & 0\\ 0 & 0 & b\end{bmatrix}\begin{bmatrix}C_l\\ C_m\\ C_n\end{bmatrix} \tag{10}$$

The aerodynamic coefficients of the GTM-T2 is composed of three parts: i) the basic airframe, ii) control surfaces, and iii) dynamic derivatives.

$$\mathbf{C} = \mathbf{C}_{\text{basic}} + \Delta\mathbf{C}_{\text{control}} + \Delta\mathbf{C}_{\text{dynamic}} \tag{11}$$

Each component is given as a 3D table with dependency on the angle of attack and the sideslip angle. The basic airframe term includes the damage model as

$$\mathbf{C}_{\text{basic}} = \bar{\mathbf{C}}_{\text{basic}} + \Delta\mathbf{C}_{\text{damage}} \tag{12}$$

In Fig. 2, the damage model of the GTM-T2 shows that how the change in the wing span affects the aerodynamic coefficients. Note that the rolling moment coefficient increment is highly dependent on the angle of attack. This

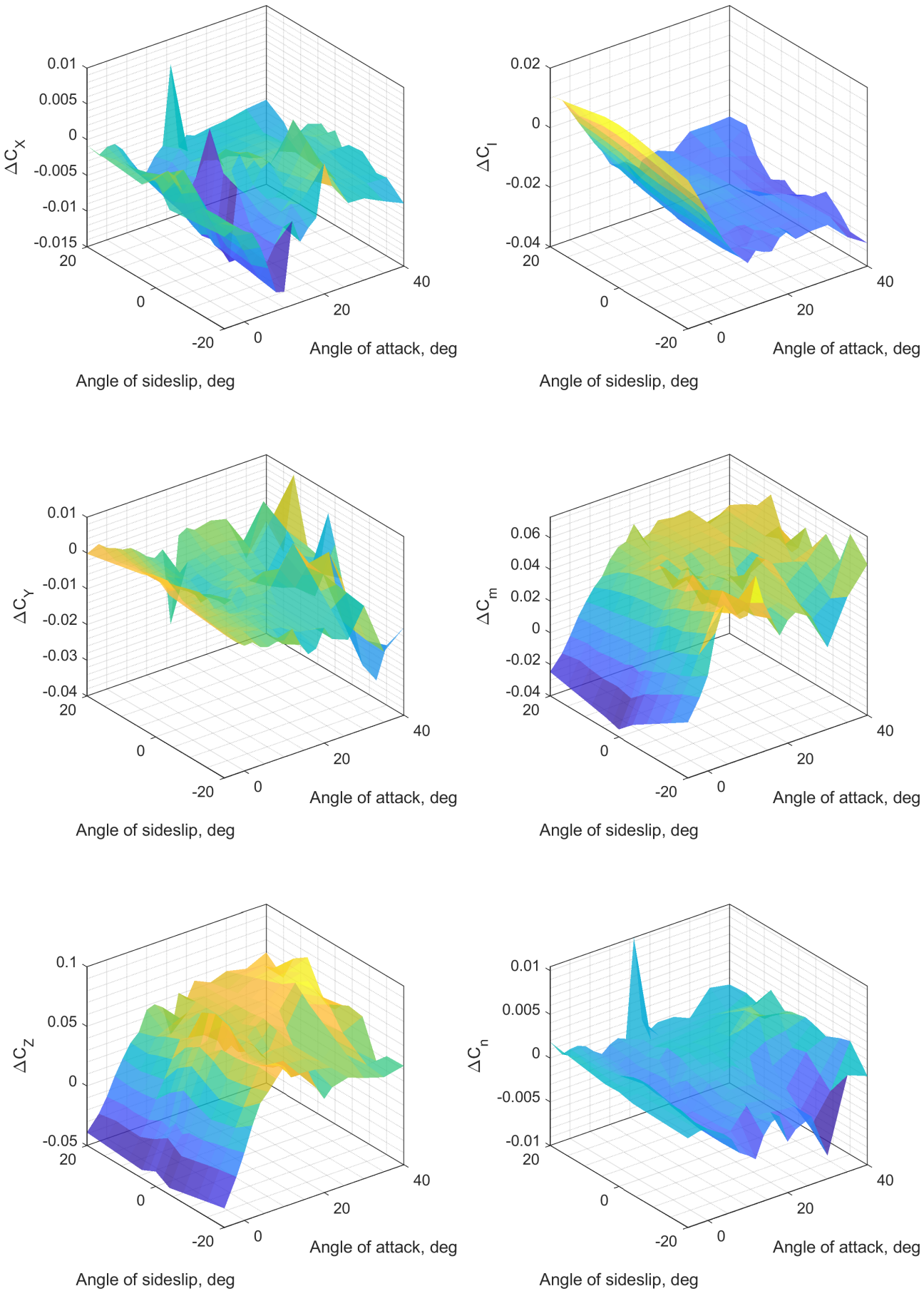

Figure 2 – Aerodynamic coefficient increment $\Delta \mathbf{C}_{\text{damage}}$ in case of the loss of the left wing tip

is because variable-span morphing generates a rolling moment by changing the lifting surface area instead of the incidence angle as in an aileron. Through linear interpolation, the aerodynamic model can be modified as

$$\mathbf{C} = \bar{\mathbf{C}}_{\text{basic}} + \Delta\mathbf{C}_{\text{control}} + \Delta\mathbf{C}_{\text{dynamic}} + \Delta\mathbf{C}_{\text{morphing}} \tag{13}$$

where the last increment $\Delta\mathbf{C}_{\text{morphing}}$ is obtained as a linear function of the morphing parameter. In this study, the quasi-static assumption is adopted, and the unsteady effect during the morphing process is not modeled because the original model does not include the unsteady effect. In Table 1, it is shown that throttle, angle of attack, and elevator deflection for the trim condition (100 knots TAS at 800 m altitude) can be changed through morphing. It shows that the symmetric morphing capability provides an additional control input for the longitudinal control channel, which enables the vehicle to adjust the throttle and the angle of attack for the same flight condition.

2.3 Engine Model

The GTM-T2 is equipped with two Jetcat P70 engines. The detailed thrust model is omitted here for brevity.

$$\begin{bmatrix} X_T \\ Y_T \\ Z_T \end{bmatrix} = \begin{bmatrix} \cos\theta_L \cos\psi_L \\ \sin\psi_L \\ -\sin\theta_L \cos\psi_L \end{bmatrix} T_L + \begin{bmatrix} \cos\theta_R \cos\psi_R \\ \sin\psi_R \\ -\sin\theta_R \cos\psi_R \end{bmatrix} T_R \tag{14}$$

Note that the engines also generate moments due to the oblique thrust axes and the gyroscopic effect of the rotors.

2.4 Mass Distribution

The variable-span morphing process involves the change in the airframe mass distribution. Therefore, the shift in the center of gravity and the increments to the moment of inertia should be modeled. From the values before and after the left wingtip loss in the damage model, the values for the intermediate positions can be calculated in an analytical manner. As a result, the shift in the center of gravity is modeled as a linear function of the morphing parameters, and the increments to the moment of inertia are obtained as a quadratic function of the morphing parameters. In fact, the variation is not so significant that it can be treated as a disturbance in the control system design.

3. Control Design

A flight control system is designed based on NDI and time-scale separation. In the control system design, asymmetric variable-span morphing is used for roll control. Using proportional–integral–derivative (PID) control, the reference derivatives to follow the reference can be found as

$$\begin{bmatrix} \dot{V} \\ \dot{\chi} \\ \dot{\gamma} \end{bmatrix}_{ref} = K_{P_1}\left(\begin{bmatrix} V \\ \chi \\ \gamma \end{bmatrix}_{ref} - \begin{bmatrix} V \\ \chi \\ \gamma \end{bmatrix}\right) + K_{I_1}\int\left(\begin{bmatrix} V \\ \chi \\ \gamma \end{bmatrix}_{ref} - \begin{bmatrix} V \\ \chi \\ \gamma \end{bmatrix}\right)dt + K_{D_1}\frac{d}{dt}\left(\begin{bmatrix} V \\ \chi \\ \gamma \end{bmatrix}_{ref} - \begin{bmatrix} V \\ \chi \\ \gamma \end{bmatrix}\right) \tag{15}$$

First, It is assumed that the engines are aligned with the body x-axis. Then, we have

$$\dot{V} = \frac{1}{\mathrm{m}}\begin{bmatrix} \cos\alpha\cos\beta & \sin\beta & \sin\alpha\cos\beta \end{bmatrix}\begin{bmatrix} X_A + T \\ Y_A \\ Z_A \end{bmatrix} - g\sin\gamma \tag{16}$$

Solving for the required thrust gives

$$T_{req} = \frac{\mathrm{m}\dot{V}_{ref} - (X_A\cos\alpha\cos\beta + Y\sin\beta + Z\sin\alpha\cos\beta) + \mathrm{m}g\sin\gamma}{\cos\alpha\cos\beta} \tag{17}$$

Table 1 – Trim conditions at different wingspan lengths.

η_s	δ_t	α	δ_e
0 %	41.66 %	2.79 deg	2.65 deg
0.5 %	42.01 %	3.16 deg	2.76 deg
1 %	43.98 %	3.60 deg	2.99 deg

Assuming small angle of attack and zero sideslip angle, we have

$$\mu_{ref} = \sin^{-1}\left(\frac{\mathrm{m}}{X_A\alpha - Z_A} V\dot{\chi}\cos\gamma\right) \tag{18}$$

$$\alpha_{ref} = \frac{\mathrm{m}}{X_A\cos\mu}\left(V\dot{\gamma} + \frac{Z_A}{\mathrm{m}\cos\mu} + g\cos\gamma\right) \tag{19}$$

If symmetric morphing is included in the velocity loop, the additional degree of freedom allows the vehicle to follow velocity commands with different angles of attack. Therefore, flight performance can be improved by harmonizing the flight path angle command and the symmetric morphing command.
Based on the reference angles, Eqs. (18) and (19) and $\beta_{ref} = 0$, we have

$$\begin{bmatrix}\dot{\mu}\\ \dot{\alpha}\\ \dot{\beta}\end{bmatrix}_{ref} = K_{P_2}\left(\begin{bmatrix}\mu\\ \alpha\\ \beta\end{bmatrix}_{ref} - \begin{bmatrix}\mu\\ \alpha\\ \beta\end{bmatrix}\right) + K_{I_2}\int\left(\begin{bmatrix}\mu\\ \alpha\\ \beta\end{bmatrix}_{ref} - \begin{bmatrix}\mu\\ \alpha\\ \beta\end{bmatrix}\right)dt + K_{D_2}\frac{d}{dt}\left(\begin{bmatrix}\mu\\ \alpha\\ \beta\end{bmatrix}_{ref} - \begin{bmatrix}\mu\\ \alpha\\ \beta\end{bmatrix}\right) \tag{20}$$

The reference angular rate to generate the reference angle rate can be found as

$$\begin{bmatrix}p\\ q\\ r\end{bmatrix}_{ref} = \begin{bmatrix}\cos\alpha\cos\beta & 0 & \cos\alpha\\ \sin\beta & 1 & 0\\ \sin\alpha\cos\beta & 0 & -\cos\alpha\end{bmatrix}\begin{bmatrix}\dot{\mu}\\ \dot{\alpha}\\ \dot{\beta}\end{bmatrix}_{ref} + T_{BV}\begin{bmatrix}-\dot{\chi}\sin\gamma\\ \dot{\gamma}\\ \dot{\chi}\cos\gamma\end{bmatrix} \tag{21}$$

Again, the reference angular rate derivatives can be found using PID control as

$$\begin{bmatrix}\dot{p}\\ \dot{q}\\ \dot{r}\end{bmatrix}_{ref} = K_{P_3}\left(\begin{bmatrix}p\\ q\\ r\end{bmatrix}_{ref} - \begin{bmatrix}p\\ q\\ r\end{bmatrix}\right) + K_{I_3}\int\left(\begin{bmatrix}p\\ q\\ r\end{bmatrix}_{ref} - \begin{bmatrix}p\\ q\\ r\end{bmatrix}\right)dt + K_{D_3}\frac{d}{dt}\left(\begin{bmatrix}p\\ q\\ r\end{bmatrix}_{ref} - \begin{bmatrix}p\\ q\\ r\end{bmatrix}\right) \tag{22}$$

In the angular velocity control design, it is assumed that the engine moments are small enough. Then, the required moments can be found as

$$\begin{bmatrix}l_A\\ m_A\\ n_A\end{bmatrix}_{req} = J\begin{bmatrix}\dot{p}\\ \dot{q}\\ \dot{r}\end{bmatrix}_{ref} + \begin{bmatrix}p\\ q\\ r\end{bmatrix}\times J\begin{bmatrix}p\\ q\\ r\end{bmatrix} \tag{23}$$

The required aerodynamic moment coefficients can be calculated from Eq. (10). If the coefficients are assumed to be linearly dependent on the control surface deflections, then the coefficients can be represented as

$$\begin{bmatrix}C_l\\ C_m\\ C_n\end{bmatrix} = \begin{bmatrix}f_l\\ f_m\\ f_n\end{bmatrix} + G\begin{bmatrix}\eta_a\\ \delta_e\\ \delta_r\end{bmatrix} \tag{24}$$

where

$$G = \begin{bmatrix}C_{l_{\eta a}} & C_{l_{\delta_e}} & C_{l_{\delta_r}}\\ C_{m_{\eta a}} & C_{m_{\delta_e}} & C_{m_{\delta_r}}\\ C_{n_{\eta a}} & C_{n_{\delta_e}} & C_{n_{\delta_r}}\end{bmatrix} \tag{25}$$

Finally, the required control surface deflections can be found as

$$\begin{bmatrix}\eta_a\\ \delta_e\\ \delta_r\end{bmatrix}_{req} = G^{-1}\left(\begin{bmatrix}C_l\\ C_m\\ C_n\end{bmatrix} - \begin{bmatrix}f_l\\ f_m\\ f_n\end{bmatrix}\right) \tag{26}$$

4. Numerical Simulation

A numerical simulation is performed to demonstrate the effectiveness of the proposed scheme, where actuator dynamics are considered. Symmetric and asymmetric morphing can be used in different loops. The asymmetric portion of span morphing can be used to initiate rolling. Therefore, the morphing aircraft can be fully controlled without the conventional roll control surface. Figure 3 shows roll rate command tracking results with asymmetric morphing as a primary roll control surface. In Fig. 3, the asymmetric morphing variable continues to vary even after the commanded roll rate is achieved. This is because the control effectiveness of asymmetric morphing is affected by the angle of attack.

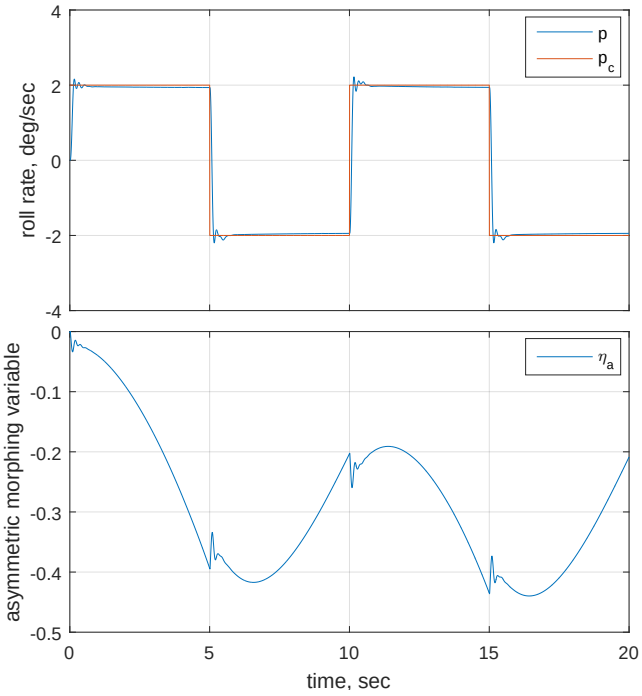

Figure 3 – Roll rate command tracking results.

5. Conclusion

In this study, a structure of the flight control system was proposed for an asymmetric variable-span morphing aircraft based on nonlinear dynamic inversion and time-scale separation. It was shown that asymmetric variable-span morphing could be used for roll control. The effectiveness of the proposed scheme was demonstrated through numerical simulation. For further study, symmetric morphing and uncertainties will be considered.

6. Contact Author Email Address

mailto: ydkim@snu.ac.kr (corresponding author)
mailto: leejihoon@snu.ac.kr

7. Copyright Statement

Acknowledgment

This work was supported by the National Research Foundation of Korea (NRF) grant funded by the Korea government (MSIT) (No. 2019R1A2C208394612).

References

[1] S. Barbarino, O. Bilgen, R. M. Ajaj, M. I. Friswell, and D. J. Inman. A review of morphing aircraft. *Journal of Intelligent Material Systems and Structures*, Vol. 22, No. 9, pp. 823–877, 2011.

[2] S. P. Joshi, Z. Tidwell, W. A. Crossley, and S. Ramakrishnan. Comparison of morphing wing strategies based upon aircraft performance impacts. *AIAA/ASME/ASCE/AHS/ASC Structures, Structural Dynamics, and Materials Conference*, Palm Springs, CA, April 2004.

[3] B. Obradovic and K. Subbarao. Modeling of flight dynamics of morphing-wing aircraft. *Journal of Aircraft*, Vol. 48, No. 2, pp. 391–402, 2011.

[4] H. M. Gracia, M. Abdulrahim, and R. Lind. Roll control for a micro air vehicle using active wing morphing. *AIAA Guidance, Navigation, and Control Conference*, Austin, TX, August 2003.

[5] M. D. Luca, S. Mintchev, G. Heitz, F. Noca, and D. Floreano. Bioinspired morphing wings for extended flight envelope and roll control of small drones. *Interface Focus*, Vol. 7, No. 1, pp. 1–11, 2017.

[6] R. Pecora, F. Amoroso, and L. Lecce. Effectiveness of wing twist morphing in roll control. *Journal of Aircraft*, Vol. 49, No. 6, pp. 1666–1674, 2012.

[7] L. Tong and H. Ji. Multi-body dynamic modelling and flight control for an asymmetric variable sweep morphing UAV. *The Aeronautical Journal*. Vol. 118, No. 1204, pp. 683–706, 2014.

[8] K. Cunningham, D. E. Cox, D. G. Murri, and S. E. Riddick. A piloted evaluation of damage accommodating flight control using a remotely piloted vehicle. *AIAA Guidance, Navigation, and Control Conference and Exhibit*, Portland, OR, August 2011.

[9] P. Lu, E. van Kampen, C. de Visser, and Q. Chu. Aircraft fault-tolerant trajectory control using incremental nonlinear dynamic inversion. *Control Engineering Practice*, Vol. 57, pp. 126–141, 2016.